







Proceedings Article

# Simulation of a modular coil unit for a preclinical MPI scanner

Jonas Schumacher <sup>a,\*</sup>, Eric Aderhold <sup>a</sup>, Pascal Stagge <sup>a</sup>, Mandy Ahlborg <sup>a</sup>, Thorsten M. Buzug <sup>a,b</sup>, Matthias Graeser <sup>a,b</sup>

<sup>a</sup>Fraunhofer Research Institution for Individualized and Cell-Based Medical Engineering IMTE, Lübeck, Germany

<sup>b</sup>Institute of Medical Engineering, University of Lübeck, Lübeck, Germany

\*Corresponding author, email: [jonas.schumacher@imte.fraunhofer.de](mailto:jonas.schumacher@imte.fraunhofer.de)

© 2024 Schumacher *et al.*; licensee Infinite Science Publishing GmbH

This is an Open Access article distributed under the terms of the Creative Commons Attribution License (<http://creativecommons.org/licenses/by/4.0>), which permits unrestricted use, distribution, and reproduction in any medium, provided the original work is properly cited.

## Abstract

The adoption of preclinical Magnetic Particle Imaging (MPI) as a standard technique in research heavily relies on the availability of scanners with a low entry barrier. One of the barriers is the infrastructure demand of such a system in terms of space, electric supply power and cooling. Scanners that try to tackle this require power-efficient transmit coil assemblies. Here, the design process of such a set of coils is presented and the optimization steps are discussed. With a total power loss of 1.2 kW for the drive and focus fields and a field of view (FoV) of 33.8 mm at 5 T m<sup>-1</sup> the whole system can potentially be powered from a single power outlet.

## I. Introduction

Modular design is a common principle in engineering. MPI scanner systems integrate multiple subsystems to achieve the goal of mapping a particle distribution into an image. One of the main modules is the set of transmit and receive coils used for signal generation and reception. Here, we present the design process of such a module with focus on the transmit coil. This module is meant for a preclinical MPI scanner with the goals of high performance and maintainability.

## II. Methods and materials

The module is simulated for a scanner system featuring a permanent-magnet-based field free line (FFL) with a gradient of 5 T m<sup>-1</sup>. The unique feature of the selection field is the shift of the FFL in a plane orthogonal to the bore axis (x-y-plane) when using a solenoid drive coil generating a magnetic field along the bore axis (z-axis). This is possible due to only having field components pointing

along the z-axis in the central x-y-plane. Since the FFL can only be shifted in the central x-y-plane, 3D imaging requires the use of a mechanical translation along the z-axis [1, 2]. Since the FoV would only be 8 mm at a drive field (DF) strength of 20 mT the scanner needs an additional focus field (FF) [3] to reach the full FoV within the free bore diameter of 40 mm. The design goals for the transmit part of the unit are as follows:

- The resulting device fits inside the existing selection field generator with a free bore of 80 mm and provides at least 40 mm final bore diameter.
- Integrates and decouples DF and FF to prevent adverse effects on either of the amplifiers used.
- Decreased power loss compared to [1] to run the system from a single power outlet.

As the DF and FF share the same direction they may influence the respective power amplifiers due to coupling or direct electrical connection. Thus, they need to be decoupled to prevent exceeding voltage ratings on one of the amplifiers. This is especially the case with the coupling from the DF to the FF amplifier due to the higher

reactance and thus higher voltages. Figure 1 shows three possible ways to implement this decoupling.

The first one is to employ a gradiometer either in the DF or FF coil which prevents high voltage induction in the FF coil by providing counteracting fields in the outer parts of the splitted coil.

The second approach is a conducting shielding tube between the DF and the FF coil. Due to the slowly changing FF, eddy currents are scarcely influencing it. On the other hand the DF with a frequency of 25 kHz is effectively blocked from inducing a voltage in the FF coil due to eddy currents.

The third variant, dubbed *combined*, uses an external bandstop filter in the FF path which is tuned to the DF frequency for the DF and FF decoupling [4]. This allows for superimposing both fields on the same coil since the DF frequency is blocked in the bandstop filter. Thus, the high voltage of the DF is prevented from adversely affecting the FF amplifier. Due to being external, the size of the filter inductors is only limited by the assigned space. Hence, it can be built with low ESR which decreases power loss in the filter. The attenuation of the DF influence on the FF amplifier is proportional to the quality factor of the bandstop filter inductor. Hence, by assigning more space to the filter the decoupling can be tuned to match amplifier safety requirements. The filter can also be extended with a low-pass section to prevent interference due the FF amplifier. This is possible since the FF frequency is only ranging up to 100 Hz and is thus significantly below the imaging bandwidth starting with the DF frequency.

Another option would be the use of a complete second unit for decoupling as proposed for receive coil decoupling in [5]. Such a unit replicates the coil setup and either has opposing turn directions or switched electrical connections for either the DF or the FF coil such that the voltages induced from DF to FF and vice versa are cancelled. This option is not considered here because it would require more connections and doubles power loss. Since this type of scanner only images a plane in the center the field is not required to be homogeneous over an extended FoV. Thus, homogeneity is not part of the following analysis.

Within the constraints of the selection field proposed by WEBER et al. [1] there is also space for multiple layers for the transmit coil with the combined approach. This can reduce the power loss due to the larger copper cross section. The selected power amplifier for the FF (A 1110-40-QE, Dr. Hubert GmbH, Germany) can supply up to 40A. Only a single unit shall be used for the FF which depending on the selected coil requires a tradeoff between power losses and FoV.

All approaches share the property that the influence of the FF on the DF amplifier is mitigated by the resonant DF path.

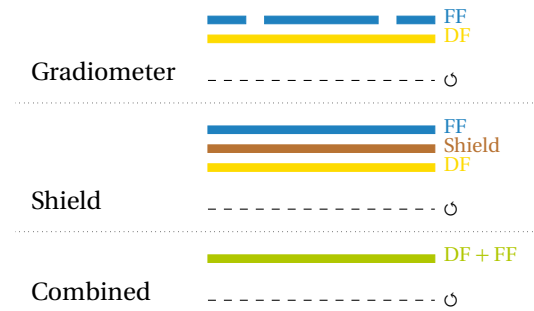


**Figure 1:** Overview of the different decoupling strategies for DF and FF. All subfigures depict a cut through the coil with the dashed line being the rotation axis.

### III. Experiments

The design process is guided by a series of simulations which will be presented in the following sections. All simulations are performed in FEMM 4.2 [6] with a DF frequency of 25 kHz and an FF frequency of 100 Hz. The simulation is run in magnetostatic mode as a 2D axisymmetric problem. The precision of for the linear solver is set to  $10^{-8}$  and an angle constraint of 30 degrees. An open boundary condition with seven layers and a radius of 200 mm is used.

#### III.1. Decoupling selection

The decoupling strategy is selected by calculating the power loss of representative geometries for the three approaches. The innermost coil always has an inner diameter of 52 mm. All simulated coils are assumed to be built with 1.6 mm  $\times$  2.6 mm square RUPALIT Profil V155 Litz wire (Rudolf Pack GmbH & Co. KG) with 1000  $\times$  0.05 mm strands. Only single-layered coils are considered for the selection. The drive field coil simulation was swepted from  $N_{DF} \in [5, 55]$  turns.

For the gradiometric FF coil with an inner diameter of 63 mm the inner part is swepted from  $N_{FF,i} \in [5, 30]$  turns with the cancellation turns on each side being  $N_{FF,c} \in [\lfloor N_{FF,i}/2 \rfloor, \lfloor N_{FF,i}/2 \rfloor + 15]$  turns. The cancellation turns allowed above  $\lfloor N_{FF,i}/2 \rfloor$  are introduced to account for lower field amplitudes at the edges of the DF coil and thus a resulting mismatch in cancellation amplitude. A gap of 2 mm between the central and the outer parts of the gradiometer and of 0.1 mm between the turns is considered. For each number of DF turns the FF coil with the lowest induced voltage from the DF is chosen. The power loss in the chosen coil is calculated and the power loss of the DF coil is added to form the total power loss.

The shield approach is simulated with a 1 mm thick copper shield of 250 mm length and an inner diameter of 60 mm. The FF coil is swepted from  $N_{FF} \in [5, 55]$  turns. Preliminary simulations showed that the shield very ef-

fectively prevents the induction of a voltage from the DF coil into the FF coil. The FF on the other hand induces only low voltages in the DF coil which also see a high impedance due to the resonant nature of the DF path. Thus, the number of FF turns can be chosen independently from the DF turns. The number of FF turns is hence determined by choosing the coil with the lowest power loss. For a consistent comparison with the other approaches the total power loss is determined for each number of DF turns by adding the previously determined minimal power loss of the FF coil to the DF power loss.

In the combined approach, the power losses of DF and FF are added for each number of turns. The power loss in the blocking filter is calculated under the assumption of a quality factor of 500 and the inductance in the parallel resonance circuit always being twice the inductance of the transmit coil.

### III.II. Layer and turn number selection

Since there is no need for a second coil plus in one case the shield, the selected decoupling method of superimposing both DF and FF on the same coil allows for more coil layers. Within the geometric constraints a maximum of four layers can be fitted with the selected Litz wire. A sweep is run varying the layers and number of turns with the combined coil having an inner diameter of 56 mm in order to have space for coolant flow. The layer with the lowest power losses is selected for a comparison of FoV and power loss depending on the number of turns.

## IV. Results

Figure 2 depicts the power losses of the three decoupling strategies. The combined approach performs best for all turn numbers and is thus selected for the subsequent analysis. In Fig. 3 the power decrease with increasing layer count can be seen. Hence, the number of layers is selected to be four. For the final selection of the number of turns, Fig. 4 compares power losses and FoV for four layers in the combined approach. The selection of the number of turns would be optimal in terms of FoV per Watt at 26 turns but a coil of 40 turns was chosen since it provides a larger FoV of 33.8 mm and the planned gradiometric receive coil can be constructed with more freedom due to the longer coil. The total power loss of the selected coil plus blocking filter is 1.2 kW.

## V. Discussion

The selection of the decoupling strategy highly influences the power loss of the module. Since the power loss is the lowest for all turn numbers with the combined approach it is selected for the implementation. Due to the low frequency of the FF, the possible low-pass section

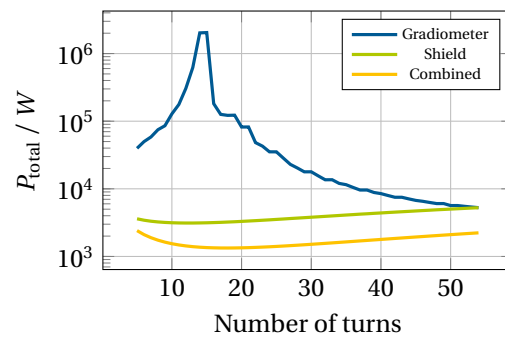


**Figure 2:** Comparison of total power loss for the different decoupling methods. The DF strength is set to 20 mT and the FF strength to 80 mT. For the gradiometer approach, the number of turns refers to the DF coil while the FF coil with the lowest induced voltage by the DF was selected for the calculation of the total power. For the shield approach the number of turns refers to the DF coil and the power of the FF coil with the lowest power losses was added to obtain the total power. For the combined approach the number of turns refers to the turns of the coil on which the DF and FF are superimposed. The power losses of the blocking filter are also considered. Please refer to section III.I for more details on the calculation of the data.

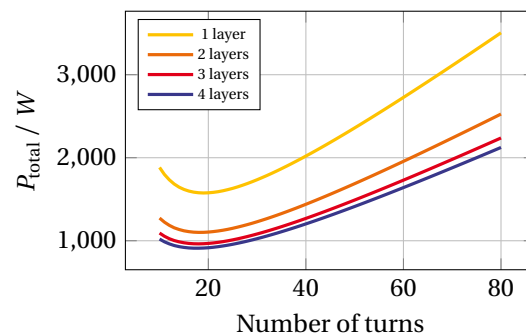


**Figure 3:** Comparison of total power loss in the combined approach depending on the number of turns. The DF strength is set to 20 mT and the FF strength to 80 mT.

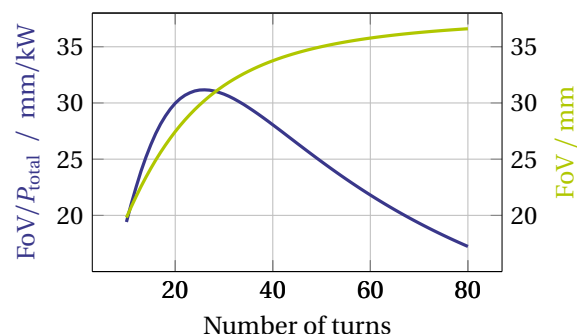


**Figure 4:** Comparison of FoV and FoV per total power loss for the four layer combined coil. The FoV is calculated based on a gradient of  $5 \text{ T m}^{-1}$ , a DF strength of 20 mT and a maximum available FF current of 40 A.

on the FF filter side and the possibility of gradiometrically decoupling the receiving coil [5], adverse effects due to interference from the FF amplifier are not to be expected with this approach. Varying the geometry like distance between gradiometer parts, shield thickness and radii in the simulations of the other approaches might reduce the power losses but sample checks showed no superior performance compared to the selected approach. The results are transferable to systems using solenoid coils since a scaling applies to all approaches similarly.

## VI. Conclusion

The simulation results prove the feasibility of powering the whole scanner from a single wall outlet. The next steps include the simulation and development of a tunable receive coil and the integration into the scanner system.

## Acknowledgments

Research funding: The Fraunhofer IMTE is supported by the EU (EFRE) and the State Schleswig-Holstein, Germany (Project: IMTE – Grant: 124 20 002).

## Author's statement

Conflict of interest: Authors state no conflict of interest.

## References

- [1] M. Weber, J. Beuke, A. Von Gladiss, K. Gräfe, P. Vogel, V. C. Behr, and T. M. Buzug. Novel field geometry using two halbach cylinders for ffl-mpi. *International Journal on Magnetic Particle Imaging*, Vol 4:No 2 (2018), 2018, doi:[10.18416/IJMPI.2018.1811004](https://doi.org/10.18416/IJMPI.2018.1811004).
- [2] E. Aderhold, J. Schumacher, P. Stagge, M. Ahlborg, T. M. Buzug, and M. Gräser, Towards a fully integrated preclinical field-free line mpi scanner, in *International Journal on Magnetic Particle Imaging IJMPI*, Vol. 9, 2023.
- [3] B. Gleich, J. Weizenecker, H. Timminger, C. Bontus, I. Schmale, J. Rahmer, J. Schmidt, J. Kanzenbach, and J. Borgert, Fast mpi demonstrator with enlarged field of view, in *Proc. Intl. Soc. Mag. Reson. Med.*, 18, 2010.
- [4] E. Aderhold, J. Schumacher, and T. M. Buzug. Co-optimisation of send and receive coils. *International Journal on Magnetic Particle Imaging*, pp. Vol 6 No 2 Suppl. 1 (2020), 2020, doi:[10.18416/IJMPI.2020.2009037](https://doi.org/10.18416/IJMPI.2020.2009037).
- [5] M. Graeser, T. Knopp, M. Grüttner, T. F. Sattel, and T. M. Buzug. Analog receive signal processing for magnetic particle imaging. *Medical Physics*, 40(4), 2013, doi:[10.1118/1.4794482](https://doi.org/10.1118/1.4794482).
- [6] D. C. Meeker, Finite element method magnetics, version 4.2. URL: <https://www.femm.info>.